MODESTUM
OPEN ACCESS

Eurasian Journal of Analytical Chemistry, 2018, 13(5), em56
ISSN:1306-3057
Research Paper https://doi.org/10.29333/ejac/95253

Synthesis of CdTiO3 Thin Films and Study the Impact of Annealing Temperature on their Optical, Morphological and Structural Properties

Ahmed K. Abass [1*]

[1] Department of Chemistry, College of Science, University of AL-Qadisiyah, Dewanyia 1753, IRAQ

Received 12 May 2018 ▪ Revised 9 July 2018 ▪ Accepted 11 August 2018

ABSTRACT

$CdTiO_3$ thin films (TF) were deposited on conductive glass substrate (ITO) at different annealing temperatures (300, 400, 500, 600) °C by a doctor building method with composition ratio (1:1) of TiO_2 and CdO. Many techniques such as: Energy Dispersive Spectroscopy (EDS), X-Ray Diffraction (XRD), Scanning Electron Microscopy (SEM), Atomic Force Microscopy (AFM) and Ultraviolet – Visible Spectroscopy (UV-Vis) were used to describe the structure, morphology and optical characteristics of prepared TF. XRD patterns show the rhombohedral structure and crystalline nature of the films. All films were nano materials according to Scherrer equation in XRD analysis. SEM images relate the homogenous films as thickly stuffed nano particles. AFM analysis demonstrated that both the surface roughness and grain size rise slightly with increasing temperature. EDS investigation approves the existence of oxygen, cadmium and titanium components with equal atomic ratios of cadmium and titanium. By application of Tauc plots, optical band gaps of CdTiO3 films are proposed to be (2.25-1.73) ev at the range of temperatures (400-600) °C.

Keywords: nano composites, thin films, metal oxide semiconductors

INTRODUCTION

In 1839, the Perovskite compounds were first found by Gustav Rose. Their name originates from a Russian L. A. Perovski. The main part in perovskite solar cells – which presented by Weber in 1978- was organo-metal halide (CH3NH3MX3) where M refers to Pb or Sn elements while X refers to halide elements may be Cl, Br or I. The major contrast was come due to the change in lattice parameter of halide [1]. Peovskite oxides which denote a type of compounds identified by the chemical formula (ABO3) which (A) refers to cations of rare earth or alkalin metals and (B) represents transition metal cation while (O) is anion of oxygen [2, 3]. **Figure 1** represents the structure of peroviskite oxide.

The bonding in these oxides is ionic in nature, and the bonds between the cations and the oxygen anions frequently assume some covalent character indicating strong hybridization amongst cation and anion orbitals. Consequently, for a qualitative comprehension of the perovskite electronic structure nearest to the Fermi level (valence and conduction band energy levels); it is helpful to consider the cations and anions in this framework regarding a molecular orbital picture in the linear combination of atomic orbitals approximation [4, 5, 6].

Perovskite oxides have essential utilizations in numerous fields recognized with the generation of energy, accumulation and energy conservation. For examples the conductors of both oxygen and proton in the fuel cells as strong electrolytes [7], in addition to their uses as ferroelectric polar and antiferroelectric non polar materials which have many applications in the energy storage [8, 9], electrocaloric materials (EC) which offer cooling technology without pollution in the liquid refrigerants [10] and as energy harvesters that provide a small amount of power in low-energy electronics applications [11].

✉ Ahmed.Kadhim@qu.edu.iq **(*Correspondence)**

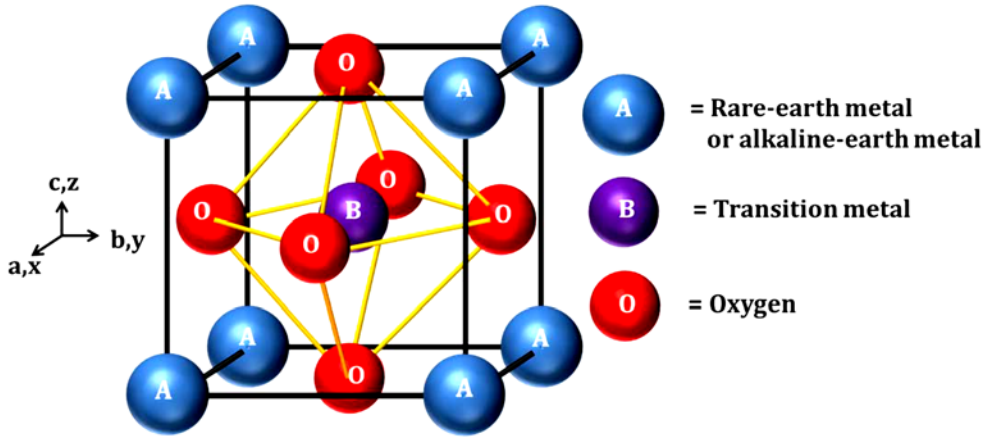

Figure 1. Structure of peroviskite oxide

Metal titanate with general formula (MTiO3; where M = Sr, Ba, Pb, Cu, Fe, Cr, Cd, and Zn) has high interest because they show magnificent dielectric [12], ferroelectric [13], pyroelectrical [14] piezoelectrical [15], magnetorestrictive [16] and electro-optical [17] attributes. Such prevalent blend of useful properties positioned them as intelligent materials for the advancement of sensors [18, 19], microelectronic devices [20, 21] and photocatalytic cells [22]. Cadmium titanate CdTiO3 is one type from this notable family possesses an extensive variety of the previously mentioned properties and has been broadly defined in the literature in crystal, TF and powder designs. The literature refers to numerous approaches to synthesis cadmium titanate material, for example, sol-gel [23, 24], solid state method [25] and electrospinning technique [26, 27] and so forth.

They normally exhibit a set of changes or transitions in the phase with temperature and pressure variables; these changes include ferroelectric transition –from spontaneous polarization- that is used in various uses, including electrical charge accumulators as capacitors, energy convertors as transducers, rectangular waveguides and optical fibers, thermal sensing materials and ferroelectric memory (RAM) [28]. CdTiO3 is uncommon composite semiconductor which has two phases (paraelectric and ferroelectric) with orthorhombic models, whereas the other types of perovskite compounds displaying a ferroelectric phase change. The paraelectric and ferroelectric phases have cubic and tetragonal structures.

At standard conditions, CdTiO3 has space group of Pnma type which orginated from repeating of TiO6 units of the perovskite skeletal in a zigzag form [29]. This model can be explained as symmetry decreasing and unit cell size increasing from one unit of cubic part to four units of orthorhombic part. CdTiO3 undergoes transition in the phase from centrosymmetric to noncentrosymmetric at 85.5 K [30– 32].

The splitting in the symmetry of the places belong to titanium and oxygen ions on the B axis which shifted towered A cations presents an dipole moment then the phase of low temperature be ferroelectric with keeping of orthorhombic symmetry. Shan et al. [33] explained that the structure of ferroelectric has symmetry of Pn21a or P21ma according to Rietveld indexing of XRD informations at 15 K. both space groups are subclasses of Pnma class. The first space group represents the vibrational mode softening of B2u type of symmetry whereas the second space group denotes the softening for B3u type [34]. The purpose of this work is synthesis nanocomposites of cadmium oxide with titanium oxide and study the effect of substrate temperature on some structural and optical constants using doctor blading method.

EXPERIMENTAL SECTION

Synthesis of CdTiO3 Powder

Cadmium iodide was from Sigma-Aldrich and titanium dioxide (anatase, TRONOX) was from Croma-Gesellschaft mbH & Co. and. CdTiO3 TF was prepared by impregnation method as follows: 2.8519 gm of CdI2 was dissolved in100 mL deionized water with vigorous stirring until complete solubility and ahomogenous solution reached. Then 1 gm of TiO_2 was put in the above solution with vigorous stirring at 60 °C for 6 hours. The above precipitant dried in oven at 120 °C over night. The dried solid precipitant was grinded in a ceramic mortar and calcined at 450 °C for 3 hours.

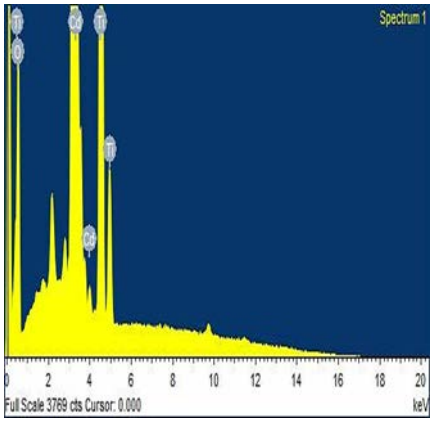

Figure 2. (EDS) spectrum of CdTiO3 TF at 300 °C

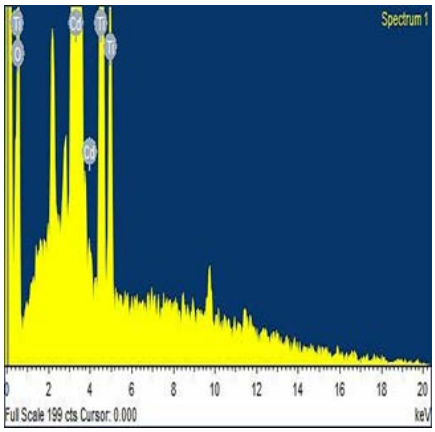

Figure 3. (EDS) spectrum of CdTiO3 TF at 400 °C

Synthesis of CdTiO3 Nanocomposite TF

The substrates used during the deposition process were ITO glass. In the beginning the substrates must be cleaned by ethyl alcohol solution and then washed by distilled water in the ultrasonicator. Substrates were then dried in an oven at 120 °C. The CdTiO3 nanocomposite TF was prepared by the doctor blading method as follows: CdTiO3 paste prepared by blending 1 gm of CdTiO3 with a mixture of 0.5 gm polyethylene glycol (PEG) and 1.5 ml deionized water in a ceramic mortar with vigorous stirring for 10 minutes. Then drops of this paste were put on the conducting face surface of ITO glass substrate. The paste was spread by means of glass rod according to the doctor blading method. After that the glass was annealed at range of temperatures (300, 400, 500 and 600) °C in the furnace.

RESULTS AND DISCUSSION

Compositional Characterization

The EDS spectra of the CdTiO3 TFs, weight and atomic percentages of Cd, Ti and O in the films toward conductive glass temperatures are illustrated in **Figures 2-5** and **Table 1**, which hint that every one of the films contains the components Cd, Ti also O with equal atomic ratio between cadmium and titanium.

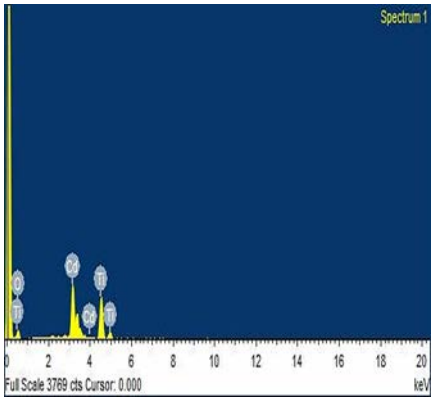

Figure 4. (EDS) spectrum of CdTiO3 TF at 500 °C

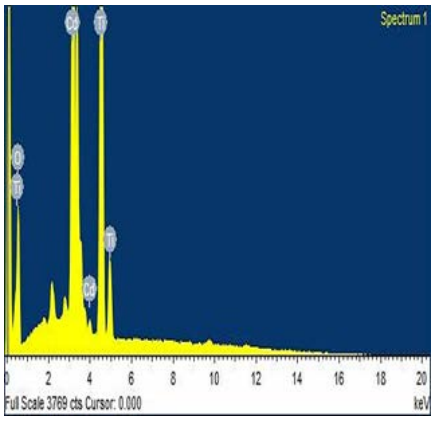

Figure 5. (EDS) spectrum of CdTiO3 TF at 600 °C

Table 1. Weight and atomic percentages of EDS analysis for CdTiO3 TFs at different annealing temperatures

Temperature (°C)	Element	Weight %	Atomic %
300	O	23.00	59.90
	Ti	23.05	20.07
	Cd	54.04	20.03
400	O	23.31	60.35
	Ti	22.9	19.82
	Cd	53.81	19.83
500	O	24.51	61.86
	Ti	22.75	19.19
	Cd	52.75	18.95
600	O	25.03	62.48
	Ti	22.71	18.95
	Cd	52.29	18.58

Structural Characterization

The x-ray diffraction spectra of CdTiO3 were checked at various annealing temperatures (300-600) °C in the extent of 2θ from 10 to 80 using 1.54 °A wavelength of Cu. The XRD diffractograms and related information describe 2θ, relative intensity and interplanar spacing for each peak, and all diffractograms had maxima position (1 0 4). **Figures 6-9** show the x-ray diffraction spectra of CdTiO3 at different annealing temperatures.

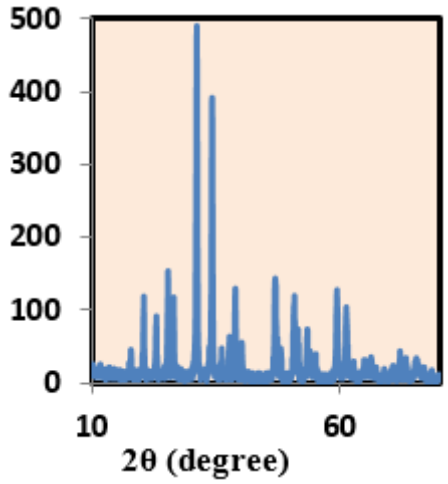

Figure 6. (XRD) diffractogram of CdTiO3 TF at 300 °C

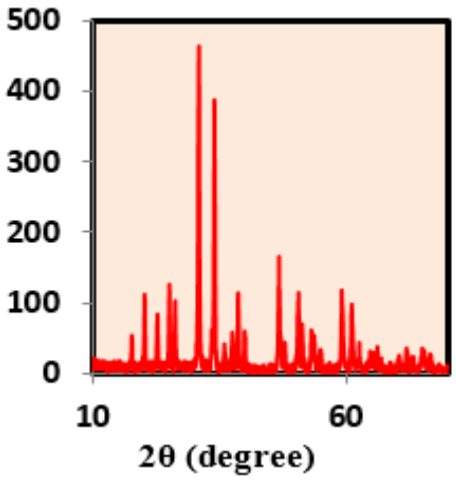

Figure 7. (XRD) diffractogram of CdTiO3 TF at 400 °C

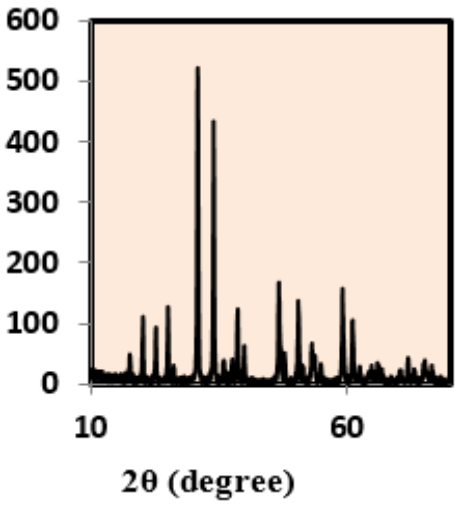

Figure 8. (XRD) diffractogram of CdTiO3 TF at 500 °C

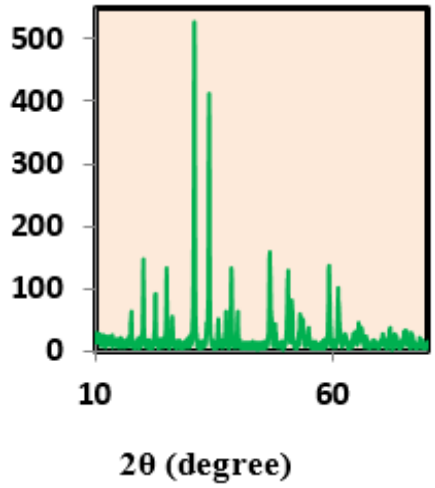

Figure 9. (XRD) diffractogram of CdTiO3 TF at 600 °C

Table 2. Lattice constants of CdTiO3 TFs at different annealing temperatures

Annealing temperature (°C)	a		c		c/a		No.unit cell	Rhombohedral		
	Observed value(obs)	Calculated value(cal)	Observed value(obs)	Calculated value(cal)	Observed value(obs)	Calculated value(cal)		a=b=c	α=β=ɣ	R. Volume
300	5.240	5.257	14.838	14.913	2.832	2.837	86212.000	5.824	53.651	118.966
400	5.240	5.243	14.838	14.844	2.832	3.594	88834.000	5.800	53.735	117.785
500	5.240	5.277	14.838	14.953	2.832	2.834	100420.000	5.842	53.703	120.224
600	5.240	6.132	14.838	15.012	2.832	2.448	91146.000	6.130	60.022	162.934

Table 3. Microstructural constants of CdTiO3 TFs different annealing temperatures

Annealing temperature (°C)	Angle position	D		Debye-Scherer Method	Williamson–Hall Method		Dislocation density
		Observed value	Calculated value	D (nm)	Ɛ	D (nm)	
300	(0 0 3)	4.9711	4.9691	35.0701	-0.0002	36.19000	0.0011
	(1 0 1)	4.3538	4.3521				
	(0 1 2)	3.8835	3.8820				
400	(0 0 3)	4.9480	4.9461	35.4458	-0.0005	32.9000	0.0010
	(1 0 1)	4.3419	4.3402				
	(0 1 2)	3.8738	3.8723				
500	(0 0 3)	4.9845	4.9825	36.1534	-0.0001	38.0947	0.00103
	(1 0 1)	4.3696	4.3679				
	(0 1 2)	3.8949	3.8934				
600	(0 0 3)	5.0040	5.0021	35.8137	-0.0003	36.1900	0.0009
	(1 0 1)	4.3824	4.3807				

It was found that all films were polycrystalline had a rhombohedral structure with space group R-3 (148). Three strongest peaks in each temperature at 2θ positions of 31.03 °C, 34.12°C and 46.83°C can be assigned to the planes (1 0 4), (1 1 0) and (0 2 4) planes of the rhombohedral structure (JCPDS Card No. 00-029-0277). In addition to these peaks, other peaks corresponding to (0 0 3), (1 0 1), (0 1 2), (1 0 4), (0 1 5), (1 1 3), (0 2 1), (0 2 4), (1 1 6), (0 1 8). (2 1 1), (1 2 2), (2 1 4), (3 0 0), (1 2 5), (1 0 1), (2 1 7), (0 1 1), (2 2 3) and (1 2 8) planes were observed in all the samples.

XRD peaks were indexed as hexagonal structures, and then converted to rhombohedral structure. The lattice and microstructural parameters are shown in **Table 2** and **Table 3** respectively. According to **Table 2**, the unit cell volume increase with increasing annealing temperature due to increasing in the grain size which lead to increase in the length of M-O bond where M is metal [35].

All lattice parameter values were estimated depending upon (0 0 3) and (1 0 1) planes at various annealing temperatures. A very little deviation from the standard values was noticed for lattice parameter which might be due to the small strain presented in the samples which means that the sample was contained only on Cd, Ti and O atoms as expressed by EDS technique. The crystallite size 'D' of the film increases slightly with increasing annealing

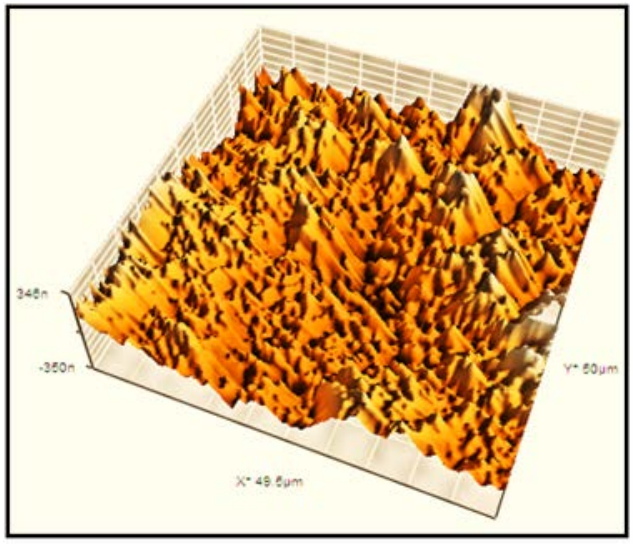

Figure 10. (AFM) micrograph of CdTiO3 TF at 300 °C

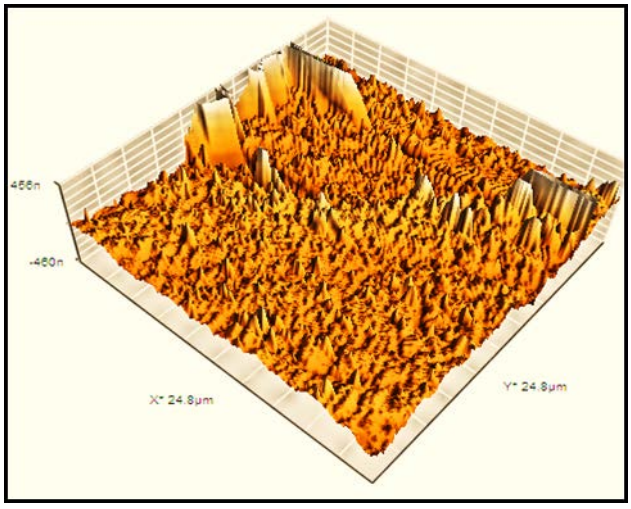

Figure 11. (AFM) micrograph of CdTiO3 TF at 400 °C

temperature. When the temperature of annealing increases, the density of the nucleation centers decreases and under these circumstances, a small number of centers start to grow, resulting in larger grains.

Surface Characterization

The surface structure of CdTiO3 TFs was examined utilizing (AFM) technique. The images of AFM for the TF annealed at (300, 400, 500 and 600) °C are shown in **Figures 10-13**. The outcomes indicate that increment in the annealing temperatures lead to the raise of the surface roughness slimly because of the grain size increasing of as in **Table 4**. This is due to the increasing in the mobility and the migration by increasing of annealing temperature.

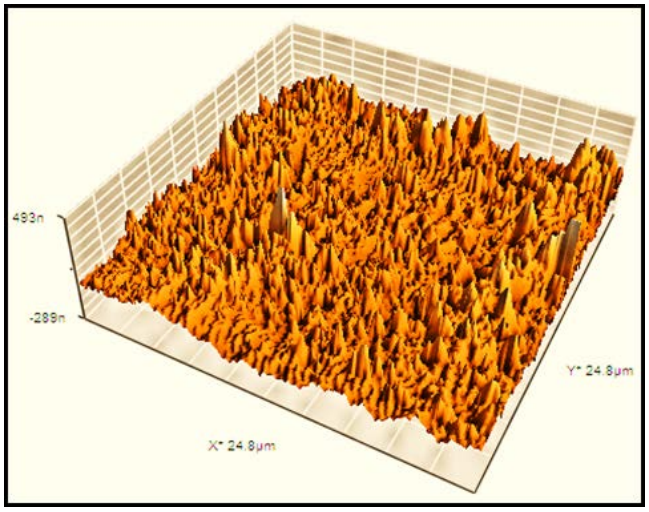

Figure 12. (AFM) micrograph of CdTiO3 TF at 500 °C

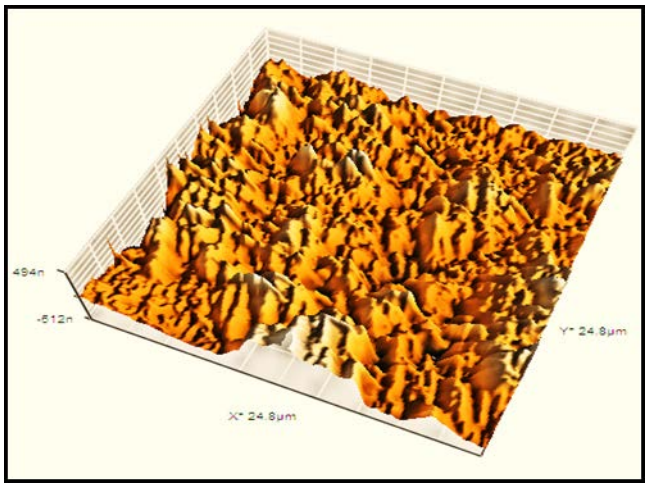

Figure 13. (AFM) micrograph of CdTiO3 TF at 600 °C

Table 4. Roughness and mean grain size of CdTiO3 TFs according to AFM technique at different annealing temperatures

Temperature (°C)	Roughness (nm)	Mean grain size (nm)
300	84.104	97
400	91.595	105
500	94.784	106
600	116.08	109

Morphological Characterization

The surface characteristics of CdTiO3 TFs at a set of annealing temperatures might have been examined by means of scanning electron microscopy technique. The SEM micrographs of CdTiO3 TFs at annealing temperatures (300, 400, 500 and 600) °C are indicated in the **Figures 14-17**. It has been observed that the films have bulk compact structures with a homogeneous surface with nanocrystalline crystallites. The surfaces of CdTiO3 TFs have porous structures and this porosity might be expected due to disappearance of water molecules in the path of the framework with annealing process. It was determined that the morphology and crystallite size have been increased slightly with increasing of annealing temperature, this means that the prepared TFs were stable at numerous temperatures.

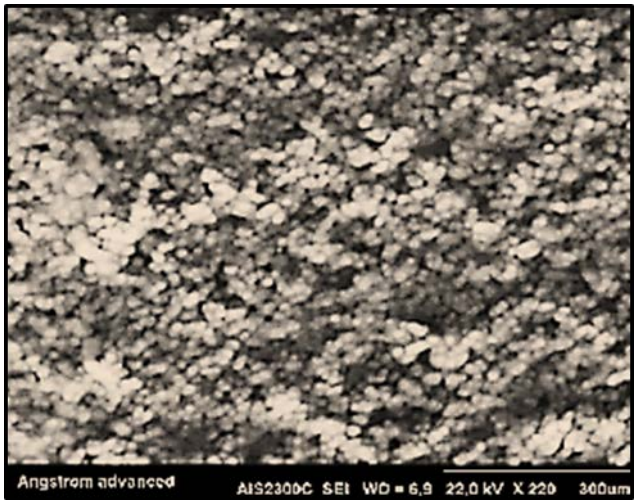

Figure 14. (SEM) image of CdTiO3 TF at 300 °C

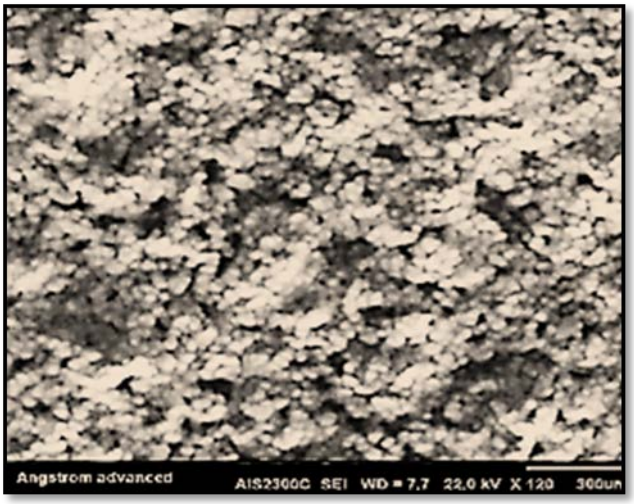

Figure 15. (SEM) image of CdTiO3 TF at 400 °C

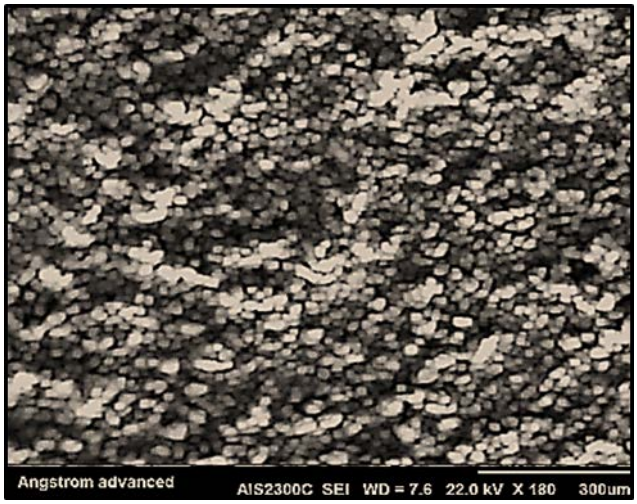

Figure 16. (SEM) image of CdTiO3 TF at 500 °C

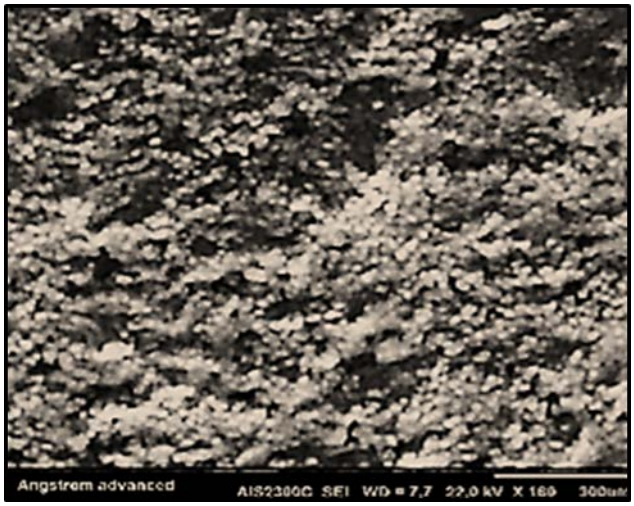

Figure 17. (SEM) image of CdTiO3 TF at 600 °C

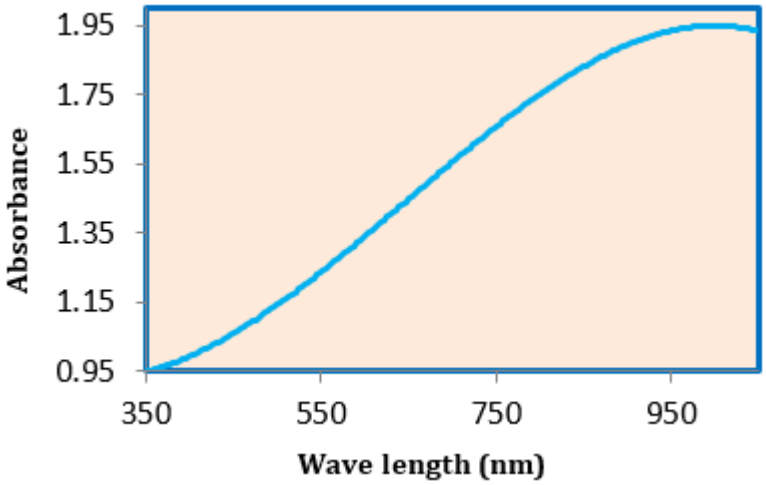

Figure 18. Electronic spectrum of CdTiO3 TF at 300 °C

Optical Characterization

Electronic spectra

The electronic spectra of the CdTiO3 TFs were described by **Figures 18-21**. The electronic spectra were gotten utilizing glass substrate as a reference. The optical properties of CdTiO3 TFs are illustrated in **Table 5**. From the **Figure 5** it can be recognized that the absorption edge exhibits a red shift due to reducing of band gap [36].

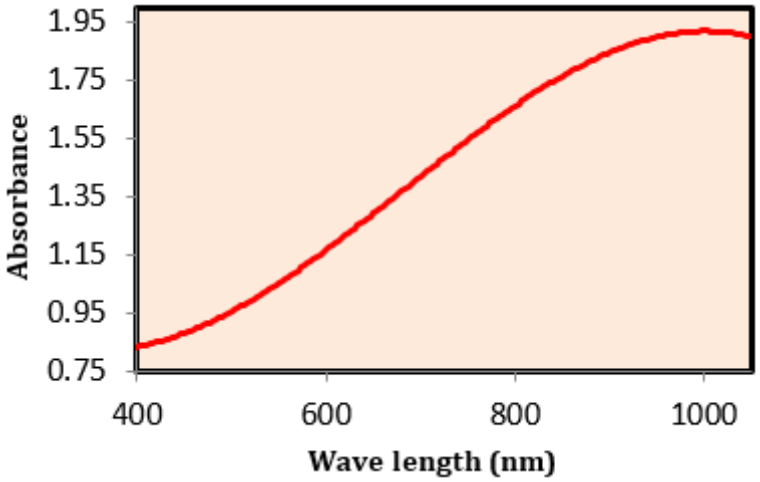

Figure 19. Electronic spectrum of CdTiO3 TF at 400 °C

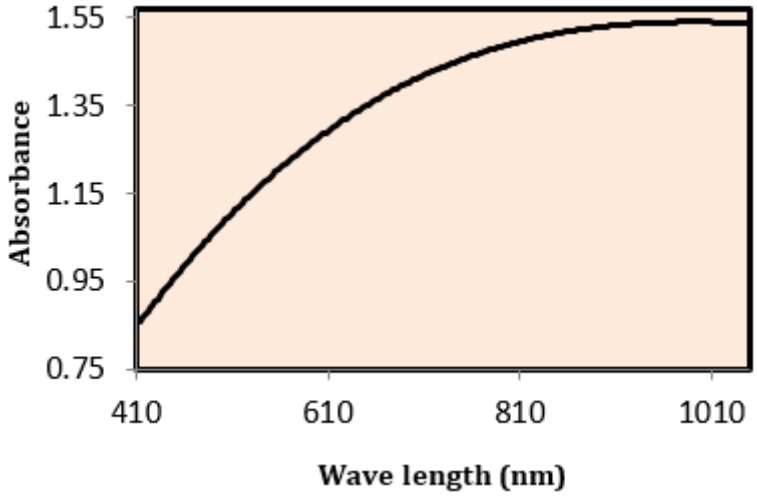

Figure 20. Electronic spectrum of CdTiO3 TF at 500 °C

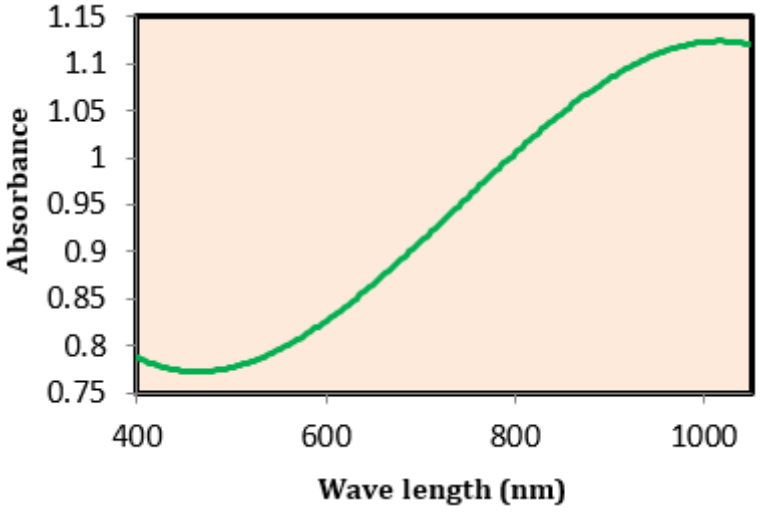

Figure 21. Electronic spectrum of CdTiO3 TF at 600 °C

Table 5. The optical properties of CdTiO3 TFs at different annealing temperatures

Temperature(°C)	Absorption coefficient (X 10^4)	Extinction coefficient	Energy gap(ev)	Optical conductivity (X 10^{14})	Real dielectric constant	Refractive index
300	4.52	0.30	1.75	2.72	6.13	2.49
400	4.88	0.35	2.25	2.97	6.28	2.53
500	4.11	0.31	1.80	2.56	6.60	2.58
600	2.97	0.21	1.73	1.73	5.87	2.43

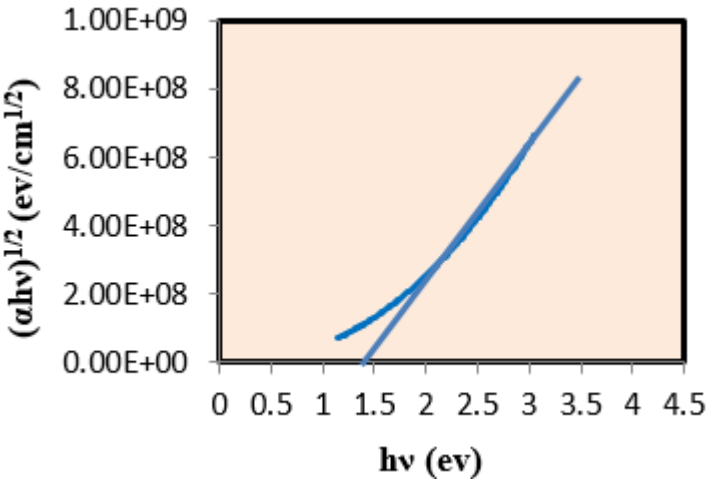

Figure 22. Energy gap of CdTiO3 TF at 300 °C

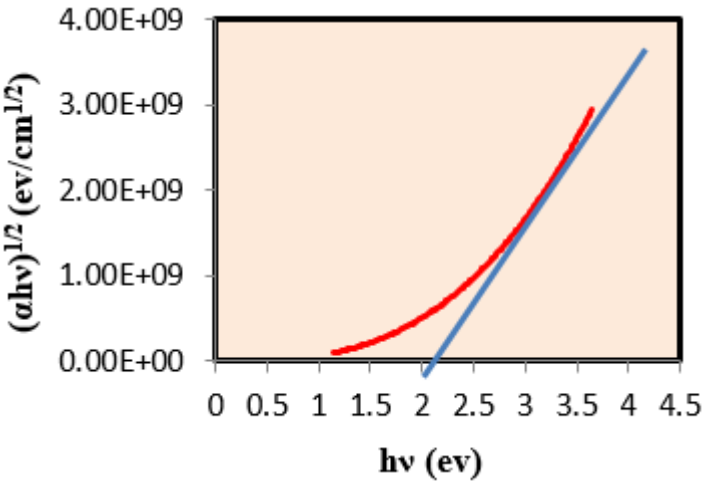

Figure 23. Energy gap of CdTiO3 TF at 400 °C

Energy gap

The electronic spectra which illustrated in **Figures 22-25** were used to extract the optical band gaps of CdTiO3 TFs. The absorption coefficient (α) can be calculated by the following equation [37].

$$\alpha h\nu = B\,(h\nu - Eg)^n \quad (1)$$

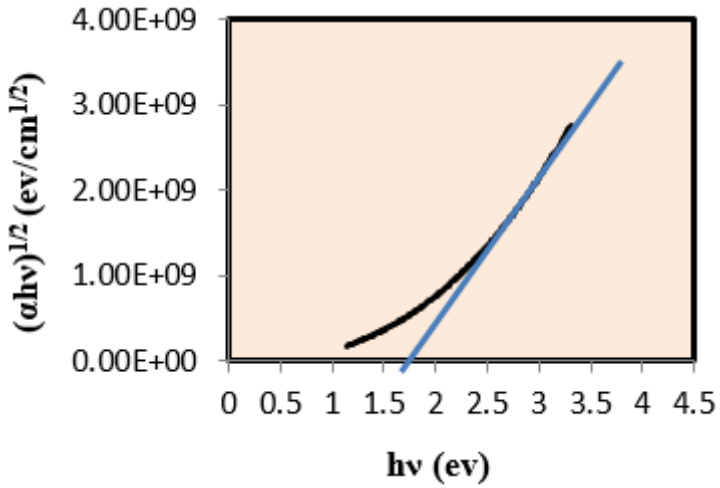

Figure 24. Energy gap of CdTiO3 TF at 500 °C

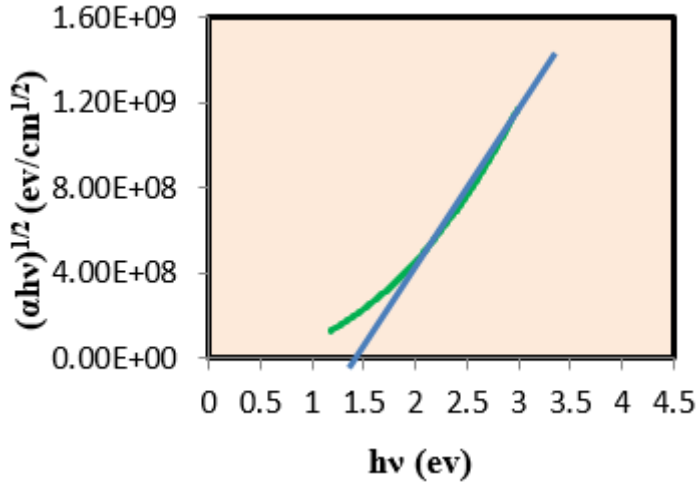

Figure 25. Energy gap of CdTiO3 TF at 600 °C

Hence (α) represents the frequency of the light, (B) is constant value depends upon the class of transition and (n) refers to the number that take certain values as (1/2, 2, 3 and 3/2) this values depend on the type of transition which direct-allowed, direct-forbidden, indirect-allowed or indirect-forbidden.

Draw of (αhv) 1/2 against hv show a direct section demonstrating that transitions must be indirect allowed transitions. The energy gap can be determined by the intercept on energy axis. The results showed that the energy gap decreases by increasing the temperature of the annealing. The outcomes suggest that the band gap energy, reduce if the substrate temperature increases. this can be due to the occurrence of new restricted levels, that are suitable to induce electrons and creation confined energy tails within the optical energy gap that take an strive at the absorption of low energy photons (deviation of the absorption edge toward lower energies) and this so prompts a decreasing of the energy gap [38].

The optical properties of CdTiO3 TFs at range of temperatures (300 - 600) °C. are illustrated in **Table 5**.

CONCLUSION

CdTiO3 TFs were deposited by employing doctor blading approach at various annealing temperatures in the range from 300 to 600 °C. The impact of glass temperature of the CdTiO3 TFs on the structural and optical features was analyzed. It was noticed that the grain growth and crystallinity of CdTiO3 TFs were increased by increasing substrate temperature. The prepared TFs were polycrystalline rhombohedral structure according to XRD analysis. The band gaps with allowed indirect type at substrate temperatures were estimated to be 2.25 to 1.73 eV. Also it was found that the band gap decrease as temperature increase.

REFERENCES

1. Jung HS, Park NG. Perovskite solar cells: from materials to devices. Small. 2015;11:10-25. https://doi.org/10.1002/smll.201402767
2. Goodenough JB, Zhou J-S. Transport properties. Localized to itinerant electronic transition in perovskite oxides. Springer. 2001. https://doi.org/10.1007/3-540-45503-5
3. Goodenough J. Electronic and ionic transport properties and other physical aspects of perovskites. Reports on Progress in Physics. 2004;67:1915. https://doi.org/10.1088/0034-4885/67/11/R01
4. Dekock RL, Gray HB. Chemical structure and bonding, University Science Books. 1989.
5. Haase W. FA Cotton: Chemical Applications of Group Theory, John Wiley & Sons Ltd., Baffins Lane 1971, p. 386. Berichte der Bunsengesellschaft für physikalische Chemie. 1972;76:173-173.
6. Burdett JK. Chemical bonding in solids, Oxford University Press. 1995.
7. Singhal SC, Kendall K. High-temperature solid oxide fuel cells: fundamentals, design and applications, Elsevier. 2003.
8. Hao X, Zhai J, Kong LB, Xu Z. A comprehensive review on the progress of lead zirconate-based antiferroelectric materials. Progress in materials science. 2014;63:1-57. https://doi.org/10.1016/j.pmatsci.2014.01.002
9. Chauhan A, Patel S, Vaish R, Bowen CR. Anti-ferroelectric ceramics for high energy density capacitors. Materials. 2015;8:8009-8031. https://doi.org/10.3390/ma8125439
10. Valant M. Electrocaloric materials for future solid-state refrigeration technologies. Progress in Materials Science. 2012;57:980-1009. https://doi.org/10.1016/j.pmatsci.2012.02.001
11. Kong LB, Li T, Hng HH, Boey F, Zhang T, Li S. Waste energy harvesting, Springer. 2014. https://doi.org/10.1007/978-3-642-54634-1
12. T Schneller T, Halder S, Waser R, Pithan C, Dornseiffer J, Shiratori Y, Houben L, Vyshnavi N, Majumder SB. Nanocomposite thin films for miniaturized multi-layer ceramic capacitors prepared from barium titanate nanoparticle based hybrid solutions. Journal of materials chemistry. 2011;21:7953-7965. https://doi.org/10.1039/c1jm10607d
13. Kingon AI, Srinivasan S. Lead zirconate titanate thin films directly on copper electrodes for ferroelectric, dielectric and piezoelectric applications. Nature materials. 2005;4:233. https://doi.org/10.1038/nmat1334
14. Ansell TY, Cann DP. High temperature piezoelectric ceramics based on (1− x)[BiScO3+ Bi (Ni1/2Ti1/2) O3]− xPbTiO3. Materials Letters. 2012;80:87-90. https://doi.org/10.1016/j.matlet.2012.04.067
15. Saito Y, Takao H, Tani T, Nonoyama T, Takatori K, Homma T, Nagaya T, Nakamura M. High performance lead-free piezoelectric material. Nature. 2004;432:84-87. https://doi.org/10.1038/nature03028
16. Ma J, Shi Z, Nan CW. Magnetoelectric Properties of Composites of Single Pb (Zr, Ti) O3 Rods and Terfenol-D/Epoxy with a Single-Period of 1-3-Type Structure. Advanced Materials. 2007;19:2571-2573. https://doi.org/10.1002/adma.200700330
17. Wang X, Xu CN, Yamada H, Nishikubo K, Zheng XG. Electro-Mechano-Optical Conversions in Pr3+-Doped BaTiO3–CaTiO3 Ceramics. Advanced Materials. 2005;17:1254-1258. https://doi.org/10.1002/adma.200401406
18. Bele A, Cazacu M, Stiubianu G, Vlad S. Silicone–barium titanate composites with increased electromechanical sensitivity. The effects of the filler morphology. RSC Advances. 2014;4:58522-58529. https://doi.org/10.1039/C4RA09903F
19. Matsubara K, Fons P, Iwata K, Yamada A, Sakurai K, Tampo H, Niki S. ZnO transparent conducting films deposited by pulsed laser deposition for solar cell applications. Thin Solid Films. 2003;431:369-372. https://doi.org/10.1016/S0040-6090(03)00243-8
20. Chan H, Choy S, Chong C, Li H, Liu P. Bismuth sodium titanate based lead-free ultrasonic transducer for microelectronics wirebonding applications. Ceramics international. 2008;34:773-777. https://doi.org/10.1016/j.ceramint.2007.09.085
21. Santander-Syro A, Copie O, Kondo T, Fortuna F, Pailhes S, Weht R, Qiu X, Bertran F, Nicolaou A, Taleb-Ibrahimi A. Two-dimensional electron gas with universal subbands at the surface of SrTiO 3. Nature. 2011;469:189. https://doi.org/10.1038/nature09720
22. Surendar T, Kumar S, Shanker V. Influence of La-doping on phase transformation and photocatalytic properties of ZnTiO 3 nanoparticles synthesized via modified sol–gel method. Physical Chemistry Chemical Physics. 2014;16:728-735. https://doi.org/10.1039/C3CP53855A
23. Mayén-Hernández S, Torres-Delgado G, Castanedo-Pérez R, Mendoza-Alvarez J, Zelaya-Angel O. Optical and structural properties of CdO+ CdTiO3 thin films prepared by sol–gel. Materials Chemistry and Physics. 2009;115:530-535. https://doi.org/10.1016/j.matchemphys.2008.11.046
24. Mohammadi M, Fray D. Low-temperature perovskite-type cadmium titanate thin films derived from a simple particulate sol–gel process. Acta Materialia. 2009;57:1049-1059. https://doi.org/10.1016/j.actamat.2008.10.040

25. Yang LY, Feng GP, Wang TX, Zhang JM, Lou TJ. Low temperature preparation and characterization of CdTiO3 nanoplates. Materials Letters. 2011;65:2601-2603. https://doi.org/10.1016/j.matlet.2011.05.090
26. Imran Z, Batool S, Israr M, Sadaf J, Usman M, Jamil H, Javed M, Rafiq M, Hasan M, Nur O. Fabrication of cadmium titanate nanofibers via electrospinning technique. Ceramics International. 2012;38:3361-3365. https://doi.org/10.1016/j.ceramint.2011.12.046
27. Hassan MS, Amna T, Khil M-S. Synthesis of high aspect ratio CdTiO3 nanofibers via electrospinning: characterization and photocatalytic activity. Ceramics International. 2014;40:423-427. https://doi.org/10.1016/j.ceramint.2013.06.018
28. Rabe KM, Ahn CH, Triscone J-M. Physics of ferroelectrics: a modern perspective, Springer Science & Business Media. 2007.
29. Sasaki S, Prewitt CT, Bass JD, Schulze W. Orthorhombic perovskite CaTiO3 and CdTiO3: structure and space group. Acta Crystallographica Section C: Crystal Structure Communications. 1987;43:1668-1674. https://doi.org/10.1107/S0108270187090620
30. Smolenski G. A New Dielectric Ceramic Based on Pb (TixZr1–x) O3. Dokl. Akad. Nauk. SSSR, 1950. 405.
31. El-Mallah H, Watts B, Wanklyn B. Birefringence of CaTiO3 and CdTiO3 single crystals as a function of temperature. Phase Transitions: A Multinational Journal. 1987;9:235-245. https://doi.org/10.1080/01411598708242352
32. Sun P-H, Nakamura T, Shan YJ, Inaguma Y, Itoh M. The study on the dielectric property and structure of perovskite titanate CdTiO3. Ferroelectrics. 1998;217:137-145. https://doi.org/10.1080/00150199808015031
33. Shan YJ, Mori H, Wang R, Luan W, Imoto H, Mitsuruitoh, Nakamura T. Powder X-ray diffraction study of ferroelectric phase transition in perovskite oxide CdTiO3. Ferroelectrics. 2001;259:85-90. https://doi.org/10.1080/00150190108008721
34. Gorshunov B, Pronin A, Kutskov I, Volkov A, Lemanov V, Torgashev V. Polar phonons and specific features of the ferroelectric states in cadmium titanate. Physics of the Solid State. 2005;47:547-555. https://doi.org/10.1134/1.1884720
35. Ridha S, Essebti D, Hlil EK. Impact of Annealing Temperature on the Physical Properties of the Lanthanum Deficiency Manganites. Crystals. 2017;7:301. https://doi.org/10.3390/cryst7100301
36. Castillo JH, Rodriguez FJ, Vigil AL-M, Sanchez-Mora E, Quiroz MA, Bandala ER. Synthesis, Structural Characterization and Photocatalytic Activity of Iron-Doped Titanium Dioxide Nanopowders. Journal of Technology Innovations in Renewable Energy. 2015;4:1-9. https://doi.org/10.6000/1929-6002.2015.04.01.1
37. Chopra KL, Das SR. Why thin film solar cells? Thin film solar cells. Springer. 1983. https://doi.org/10.1007/978-1-4899-0418-8
38. Salman SA, Khodair ZT, Abed SJ. Study the Effect of Substrate Temperature on the Optical Properties of CoFe2O4 Films Prepared by Chemical Spray Pyrolysis Method. 2015.